Cement and Concrete Research 39 (2009) 313–323

Contents lists available at ScienceDirect

Cement and Concrete Research

journal homepage: http://ees.elsevier.com/CEMCON/default.asp

Quantitative distribution patterns of additives in self-leveling flooring compounds (underlayments) as function of application, formulation and climatic conditions

A. De Gasparo [a,*], M. Herwegh [a], R. Zurbriggen [b], K. Scrivener [c]

[a] Institute of Geological Sciences, University of Berne, Switzerland
[b] Elotex AG, Sempach Station, Switzerland
[c] Laboratory of Construction Materials, EPFL, Switzerland

ARTICLE INFO

Article history:
Received 6 June 2008
Accepted 16 December 2008

Keywords:
Mortar
Additives
Polymers
Microstructure gradients

ABSTRACT

The distributions of organic additives in self-leveling flooring compounds (SLCs) were investigated using laser-scanning microscopy for the selective visualization of the additives, which had been previously stained by a fluorescent dye. The distributions of latex (VC), polycarboxylate ether (PCE), cellulose ether (CE), casein (Cas) and polyvinyl alcohol (PVA, a component of redispersible powders) were analyzed in Portland (PC) and Calcium aluminate cement (CAC) dominated SLC formulations as a function of application thickness and different climatic conditions. It is shown that evaporation induced water flux through the communicating pore system causes considerable enrichments of these additives in the uppermost millimeter of the mortar layer. The resulting fractionation factors can be correlated with the different hydration kinetics of PC or CAC dominated mixed binders as well as with the drying conditions. Investigations on the additive distribution indicate that CAC dominated formulations develop more homogeneous enrichments than PC dominated systems.

1. Introduction

Self-leveling compounds (SLC; also called underlayments) are low viscous mortars, which are hand-applied as thin layers of 1–10 mm on any type of floor substrate (e.g. concrete, screed). The purpose of applying SLC is to produce a smooth and even substrate, on which the final covering such as a carpet or parquet can be applied. SLCs are delivered as dry mortars to the construction site, where they have to be mixed with a predefined amount of water to obtain a ready-to-use mortar. To fulfill all requirements of self-leveling, early setting and final properties, a SLC contains at least 10 different components plus water. Among these components a number of organic additives are required to provide the workability properties [1]. Table 1 shows the composition of the used mortar formulations. The most important additives are the superplasticizers casein (Cas) or the synthetic polycarboxylate ether (PCE), which provide flow and leveling properties; cellulose ether (CE), a stabilizer; polyvinyl alcohol (PVA) as a component of the redispersible powder (redispersion aid) and vinyl chloride terpolymer latex (VC) as the main component of the redispersible powder. A vinyl chloride terpolymer was taken for the purpose of localisation of the latex by chlorine mapping. The redispersible powder enhances flow properties, flexural strength and surface abrasion resistance. In addition retarders are required, because otherwise the setting of mixed-binders would occur much too fast. On the other hand, accelerators are added to improve the gain in early strength. The superplasticizers (casein or a synthetic superplasticizer) act as water reducing agents and provide flowing and leveling properties. The defoamer reduces the air content, which finally increases compressive strength. A low quantity of stabilizer prevents the mortar from sedimentation and bleeding, which would negatively affect material properties. The redispersible powder is mainly a strength promoter to improve final flexural strength properties. For fast curing, SLCs are based on a mixed-binder system (Calcium aluminate cement (CAC), Portland cement (PC), Calciumsulfate (C$)), which provides high final strength [2–5]. The high surface/volume ratio makes drying a key parameter. The water/cement ratio is relatively high (w/c 0.7), compared to common concrete (w/c 0.4–0.6). In light of the impact of organic additives on the properties of fresh slurries and cured mortars, empirical tests are usually performed. Self-leveling compounds are tested for their flow ability (rheological fresh mortar property) according to EN12706. With respect to the properties of the hardened mortar there is no specific industrial standard for SLCs. Therefore testing of the physical properties of a hardened SLC is carried out according to standards for screeds such as EN13813 and EN13892.

In terms of the organic additives, empirical lab tests provided in the past knowledge on the impact on the physical properties and their interaction with the cement phases for fresh mortars and for final cured mortars [4,19]. Many previous investigations dealt with the influence of organic additives on the cement hydration. Plank and Winter [6], Plank et al. [7], and Hirsch et al. [8], for example, describe

* Corresponding author.
E-mail addresses: adg@geo.unibe.ch (A. De Gasparo), roger.zurbriggen@elotex.com (R. Zurbriggen).

0008-8846/$ – see front matter © 2008 Elsevier Ltd. All rights reserved.
doi:10.1016/j.cemconres.2008.12.009

Table 1
Composition of the used SLC dry mix formulations: Portland cement dominated with casein (Pc-c) or polycarboxylate ether (Pc-p), Calcium aluminate cement dominated with casein (Cac-c) or polycarboxylate ether (Cac-p).

Component		Function	Model mortar	Pc-c	Pc-p	Cac-c	Cac-p
Portland cement		Binders	**0.00**	**26.00**	**26.00**	4.00	4.00
Calcium aluminate cement			**0.00**	10.00	10.00	**20.00**	**20.00**
C$ α-hemihydrate			**0.00**	4.00	4.00	7.00	7.00
Calcium hydroxide						0.50	0.50
Quartz sand		Fillers	43.60	43.60	43.60	36.65	36.63
Calcite powder			53.05	13.05	13.35	27.95	28.15
Organic Additives	Casein	Flow	**0.40**	**0.40**		**0.30**	
	Polycarboxylate ether				**0.10**		**0.12**
	Retarder	Retardation	0.25	0.25	0.25	0.25	0.25
	Accelerator	Early strength				0.20	0.20
	Defoamer	Densification	0.10	0.10	0.10	0.05	0.05
	Cellulose ether	Stabilization	0.10	0.10	0.10	0.10	0.10
	Redispersible powder	Strength, workability	2.50	2.50	2.50	3.00	3.00
Mixing water			23.00	23.00	23.00	23.00	23.00

The CAC-dominated formulations were taken from Bier Th. A. & Amathieu L. (1997): Calcium aluminate cement (CAC) in building chemistry formulations. Lafarge Aluminates Technical Paper F 97. Presented at the CONCHEM congress 1997 and slightly adapted to our raw materials. Note that the model mortar contains no cementitious phases. Quantities are given in wt.% on the dry mix.

the interaction of superplasticizers with cements. It was found that organic additives adsorb on cementitious phases and generally reduce cement hydration [9,10]. Wang and Zhang [11] show that, particularly CE enhances the water retention of the fresh mortar and some physical properties of the cured mortar. CE decelerates further the hydration kinetics of PC more than of CAC. This effect is dependent on the concentration and the structure of the CE [12]. Dimmig [13] investigated the morphology and distribution of organic additives in mortars. It has also been reported that latex reduced the amount of calcium hydroxide and changed the morphology of AFt and Afm [14,15]. Rozenbaum et al. [16] describes a decreasing effect of latex on the capillarity and porosity in the cement matrix. Note however, that most of these investigations were carried out on Portland cement based systems [28] and not in mixed binder systems like SLCs. According, for example, to Amathieu et al. [2], Bier and Amathieu [3], and Kighelman et al. [17] ettringite is the main phase formed in such mixed binder formulations. Synchrotron X-ray diffraction indicates ettringite crystallization immediately after the cement–water contact [18]. Jenni et al. [20,21] investigated the distribution of latex, PVA and CE in much simpler formulations of cured tile adhesive mortars. Latex was detected by element mapping and the water-soluble polymers were stained by a fluorescent dye (prior to mortar mixing) and then selectively visualized by laser scanning microscopy (LSM). The experiments of Jenni et al. [20] revealed that certain organic additives (e.g. CE) are locally enriched due to different directions of water migration during the evolution of the mortar. In case of SLCs, however, such studies are missing so far.

In this work, we try to close this gap by visualizing and quantifying the distribution of latex (vinyl acetate/ethylene/vinyl chloride terpolymer (VC)), polycarboxylate ether (PCE), cellulose ether (CE), casein (Cas) and polyvinyl alcohol (PVA, component of the redispersible powder) and the changes in their distributions as function of the evolving microstructures of the SLC mortar layers. In a second part, the processes and influences, which control the distribution of organic additives, will be investigated and discussed. For this reason, conventional and in-situ experiments, were performed under different climatic curing conditions. These experiments in combination with the use of different formulations, i.e. with Portland cement (PC) or Calcium aluminate cement (CAC) predominance, allowed the investigation of the distributions of the organic additives as a function of (i) the predominance of PC or CAC, (ii) the application thickness, and (iii) different climatic conditions and discuss their relevance along these steps.

2. Materials and sample preparation

The formulations used in this study are given in Table 1. To allow selective visualization of polycarboxylate ether (PCE), polyvinyl alcohol (a component of common redispersible powders), cellulose ether and casein, the original additives were stained prior to mortar mixing with fluorescein-5-isothiocyanate isomer I (FITC), according the procedure described by Jenni et al. [20]. Tests with mortars containing the stained additives showed that they did not change the properties of the additives and moreover, the FITC was not detached from the additive during mortar evolution. In this way, the FITC concentration directly reflects the spatial distribution of the corresponding additive within the mortar matrix [20]. As is mentioned in the work of De Gasparo [1], the interaction between cementitious mortar water and the FITC can reduce the fluorescence intensity in wet environments. This artifact affects in-situ fluorescence during early stages of mortar curing. To evaluate this effect, a model mortar without cementitious phases was used in addition to the real formulations as an analogue material (Table 1), where the cementitious phases were substituted by calcite powder with similar grain size distribution as covered by the cement phases in case of the real formulations.

2.1. Mixing procedure and mortar application

According to an ELOTEX-internal working procedure, 100 g of dry mix were mixed with the appropriate amount of water. The mixing schedule was as follows: 45 s of intense mixing (propeller stirrer, ~900 rpm), recovery of the fresh mix for at least 3 min ("time of maturation" to assure proper dissolution and dispersion of the components) followed by manual mixing with a spatula for another 15 s. Afterwards the fresh slurry was immediately poured onto an unprimed cement fiber-board (Eternit) resulting in an approximate thickness after spreading of 4 mm. Some specific samples were applied in layers with thicknesses of ~20 mm (see below).

2.2. Sample preparation for microscopy

Confocal laser scanning microscopy (LSM) and electron microscopy required specific sample preparations. For confocal LSM, it is essential to collect fluorescence signals within a planar 2-D section. For samples, which are exposed to water during the preparation procedure, a prior impregnation is inevitable. Otherwise wet sawing and polishing would provoke additional hydration of only partially hydrated cement grains and dissolution of some of the polymeric phases. Furthermore, impregnation prevents a mechanical destruction of delicate microstructural features by abrasion products generated during sawing and polishing. In case of the LSM samples, impregnation was done by polyfin, which avoids reactions between impregnation resin and organic additives [22]. For more detailed information in terms of sample preparation see [1]. Note that all samples taken from the final hardened mortar represent sections perpendicular to the mortar surface.

3. Methods and instrumental set-up

3.1. Laser scanning microscopy

Laser scanning microscopy investigations (Zeiss, LSM 410) were performed over the entire cross-section areas (~4–23 mm thick layers) from mortar surfaces to mortar base to detect the distribution of FITC stained polycarboxylate ether (PCE), cellulose ether (CE), casein (Cas) and polyvinyl alcohol (PVA). The LSM settings were kept identical for all

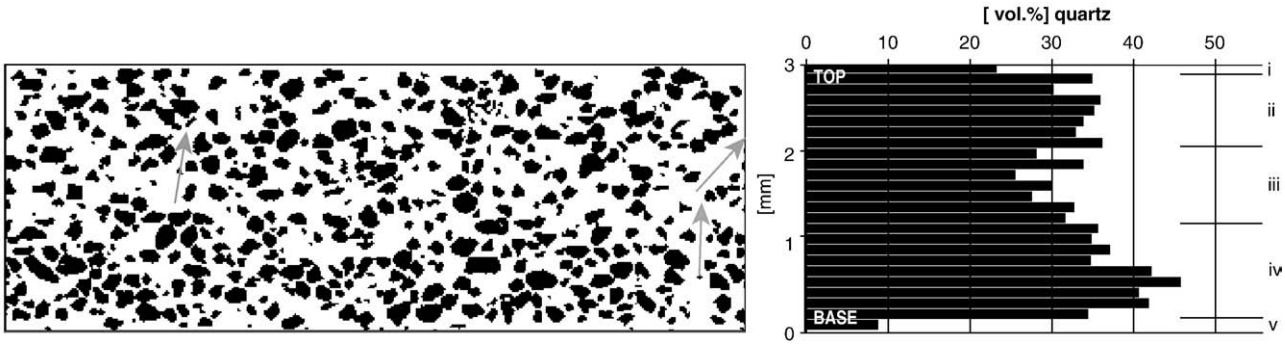

Fig. 1. Quartz grain distribution in a 3 mm thick Pc dominated SLC layer. The left picture shows a binary picture of the segmented quartz grains. The right picture shows the corresponding quartz grain distribution pattern.

samples and were as follows: confocal mode, lens: 6.3/0.25, image size: 512×512 pixels, pixel size: 2.646 µm, wavelength of the laser: 488 nm, scan time: 2 s, confocal/average: 4, attenuation: 1/100, bandwidth: 0, contrast: 292, brightness: 9816, pinhole: 100, and zoom: 1.5. To image an entire mortar section, image mosaics consisting of 4 to 25 rows and 4 to 10 columns were acquired and matched afterwards.

3.2. In-situ observations of the mortar surface

To investigate the surface enrichment process of water-soluble polymers like cellulose ether (CE), casein (Cas) and polyvinyl alcohol (PVA) as a function of different climatic conditions, time resolved in-situ observations of the mortar surface were performed under different climates [1]. These experiments were carried out with Portland cement dominated and model mortar formulations (Table 1). For this purpose, a climate box, equipped with temperature and humidity measurement devices, was developed [1]. Three different measurement set-ups were applied: (i) normal curing at room temperature (~23 °C and 50% rel. humidity), (ii) curing under hot-dry air flux (~50 °C) and (iii) curing at room temperature with 100% rel. humidity in the climate box. For these in-situ investigations, the fresh slurry was applied in 4 mm thick layers on a cement fiber-board (area: 40×30 mm), which was positioned directly under a binocular microscope (Leica Wild M10). The equipment consisted of a SONY DFW-X700 digital camera, plane light (100 W) and UV light (Philips bulb, 100 W, H44JM-100, mercury flood) for illumination. The following measurement parameters were used: magnification: 10, lens: 0.63, aperture: 1. Camera settings: brightness: 55, gain: 74, sharpness: 7, hue: 45, saturation: 128, gamma: 1, shutter: 210, blue gain: 128, and red gain: 140. To avoid measurement artifacts like bleaching of the FITC, it was important to protect the sample from daylight. Therefore, the experiments were carried out in a fume cabinet that was shielded against light and the sample was illuminated by fluorescent and/or plane light only during 10 seconds for image acquisition (imaging interval of 30 min). Furthermore, the angles of illumination and direction of flux of hot-dry air were kept constant. Temperature and humidity were measured every 10 min. Additionally, cross-sections perpendicular to the mortar surface were investigated on the finally cured and cut samples with a laser-scanning microscope (LSM; see 3.1).

3.3. Digital image analysis

Image processing and analysis were carried out with Photoshop 7.0 and Image SXM 174-1X (freeware: Steve Barrett, www.liv.ac.uk/~sdb/ImageSXM/; dato 30.01.2009). Due to the low amount present, the concentration of the stained organic additives was directly proportional to the fluorescence intensity (FI) [23]. In this way, we used the measured grey value in the finally investigated picture as an indicator of the amount of additive present locally. Scanning of the laser beam and simultaneous signal detection therefore allowed spatially resolved polymer distributions to be obtained. Jenni et al. [20] developed an analysis routine that calculates the grey value intensity of the fluorescing additive for a user defined number of horizontal stripes, for which the fractionation factor (total FI of a stripe/(total sum of FI of the entire sample/number of stripes)) was calculated. In this sense, fractionation plots over the mortar section were derived. For the analysis of surface fluorescence, the green channel was extracted from the original TIFF color image using Adobe Photoshop. This step is necessary, because transformation of the original polychromatic color-images into a monochromatic 255 grey value look up table delivers grey values not uniquely defined by a specific color. Based on the resulting

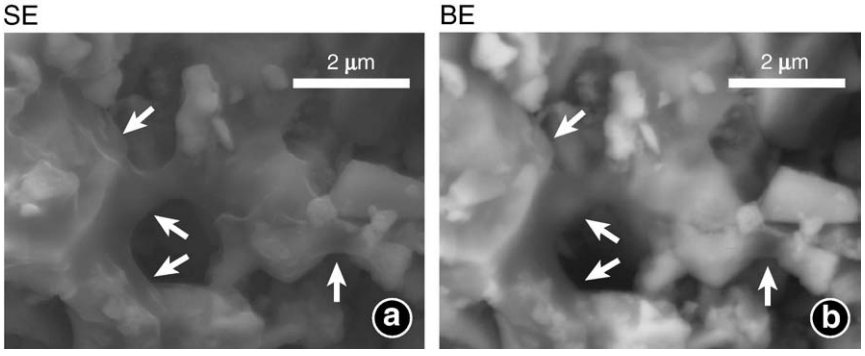

Fig. 2. Secondary electron (SE) and back-scattered electron (BE) images of fracture surfaces of SLC formulations: polymer sails and menisci-like structures represent organic additive structures (see arrows in a, b). In the BE image they loose their distinct contours or turn dark due to their low atomic weights.

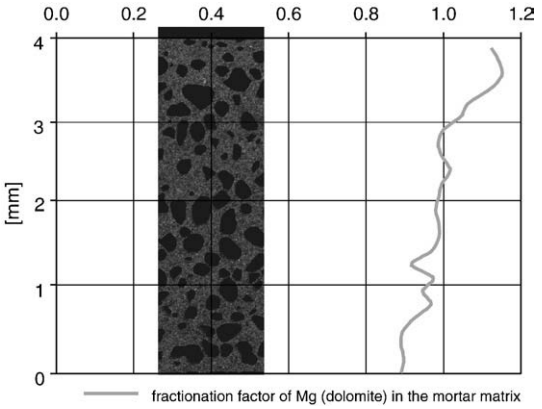

Fig. 3. Element mapping of Mg (right part) representing the distribution of dolomite (left part) as fine filler in the matrix: within the data scatter, note the maximal difference of 0.25 between the fractionation factor at the mortar base (0.9) and the mortar top (1.15). For electron microprobe analyzer (EMPA) measurement settings see [20].

gray-value image, rectangular stripes were selected for which the mean grey values were extracted with image SXM representing the average fluorescence intensity (FI). See [20,24,1] to obtain more detailed information with respect to the applied methods to obtain additive distributions in the mortar.

4. Results

4.1. Distribution of quartz sand in the SLC layer

There are five horizontal zones of distinct quartz concentrations (Fig. 1). (i) At the top quartz sand is depleted. (ii) Then a ~1 mm thick zone of a mean quartz concentration occurs. (iii) Nearly in the middle, quartz is depleted (iv) to become gradually enriched downwards. (v) In contact to the flat substrate, the coarse quartz grains are depleted again. Another striking feature is the local appearance of vertical or inclined channels consisting of matrix material only (see arrows Fig. 1).

4.2. Microstructures related to organic additives

Due to the dense packing of the very fine-grained matrix components and the resulting capillary pores in micron and sub-micron range, the size of the polymeric microstructures is very small. Therefore, well-developed sail-like additive films of dimensions of 1 to 3 μm are relatively rare in real mortars, but can occasionally be seen as menisci between mineral grains (Fig. 2). Other typical polymeric microstructures are very fine ridge-like structures (Fig. 2), which appear often together with thin films covering the mineral surfaces. Such films can cover the cementitious phases over areas of ~10×10 μm (Fig. 2). The most common structures are composite films consisting of organic additives, cement phases and fine fillers as they were previously described by Jenni et al. [21] for ceramic tile adhesive. Polymer films, which are transparent for back-scattered electron signals, were rare indicating that most films are of composite character or the films were simply too thick and, therefore, did not allow back-scattered electrons to transmit. Damage induced by the electron beam [27] was not observed.

4.3. Additive distribution in the matrix of PC and CAC dominated mortars

The goal of these experiments was to study if the cement type or the application thickness influence the distribution of the additives. For this reason, 4 mm and ~20 mm thick PC dominated and 4 mm thick CAC dominated mortar layers were analyzed by LSM.

To test the distribution of fine filler in the mortar layer, conventional calcareous fine filler was replaced by a similarly grained dolomitic ($CaMg(CO_3)_2$) powder, whose spatial distribution can be investigated by a magnesium element mapping in the SEM. Within the data scatter, the distribution of the dolomite was slightly enriched from bottom to top (enrichment factor from bottom to top: 0.25) within the matrix (Fig. 3). As fractionation factors of other organic additives (see Figs. 4–11; Table 2) are much higher than 0.25, the processes responsible for this irregularity cannot fully account for the organic additive enrichments described in more detail below.

Generally the additives in the 4 mm thick PC dominated layers (Figs. 4, 5, 6d–e, 7d–e and 8d–e) are more enriched towards the mortar surface than in the corresponding 4 mm thick CAC dominated layers (Figs. 6–8, always f and g). For the thick layers, the surface enrichment of cellulose ether and polyvinyl alcohol is higher (Figs. 6 and 7a–c) than in the corresponding thin layers. Casein shows a conspicuous weaker surface enrichment in the thick sample (Fig. 8a–c) than in the thin one.

Thick (~20 mm) and thin (4 mm) PC and CAC dominated mortar layers show three distinguishable distribution zones: (i) the topmost 10 to 20 μm thick skin at the mortar surface, containing the highest organic additive concentration. Note that to detect the strong enrichments in the thin skin, the topmost zone was additionally quantified with a higher resolution of the analysis stripes (Figs. 4–8). (ii) The upper part (~1 mm) of the mortar layer (just below the skin)

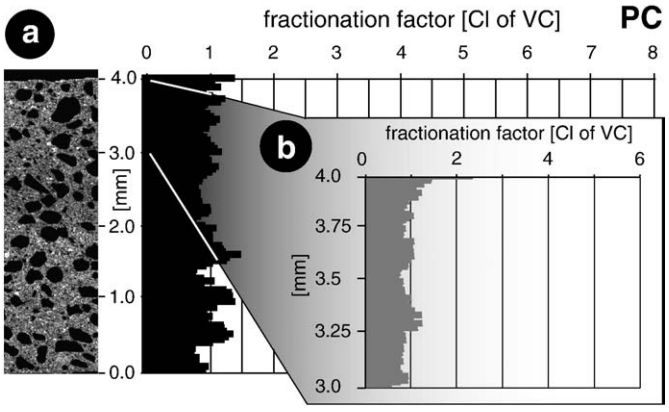

Fig. 4. (a) Distribution pattern of chlorine of the vinyl chloride terpolymer within a cross section, which is oriented perpendicular to the SLC surface. Black bars represent quantitative additive distributions (1 stripe is ~42 μm thick). The inset (b) with grey bars shows, relative additive distributions at higher resolution within the uppermost millimeter of the mortar layer (1 stripe is ~10 μm thick).

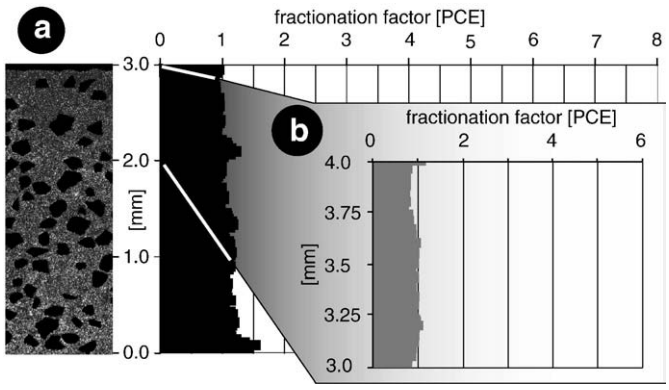

Fig. 5. Distribution pattern of polycarboxylate ether within a cross section through a PC-dominated SLC, which is oriented perpendicular to the SLC surface. Black bars represent quantitative additive distributions (1 stripe is ~42 μm thick). The inset with grey bars show, relative additive distributions at higher resolution within the uppermost millimeter of the mortar layer (1 stripe is ~10 μm thick).

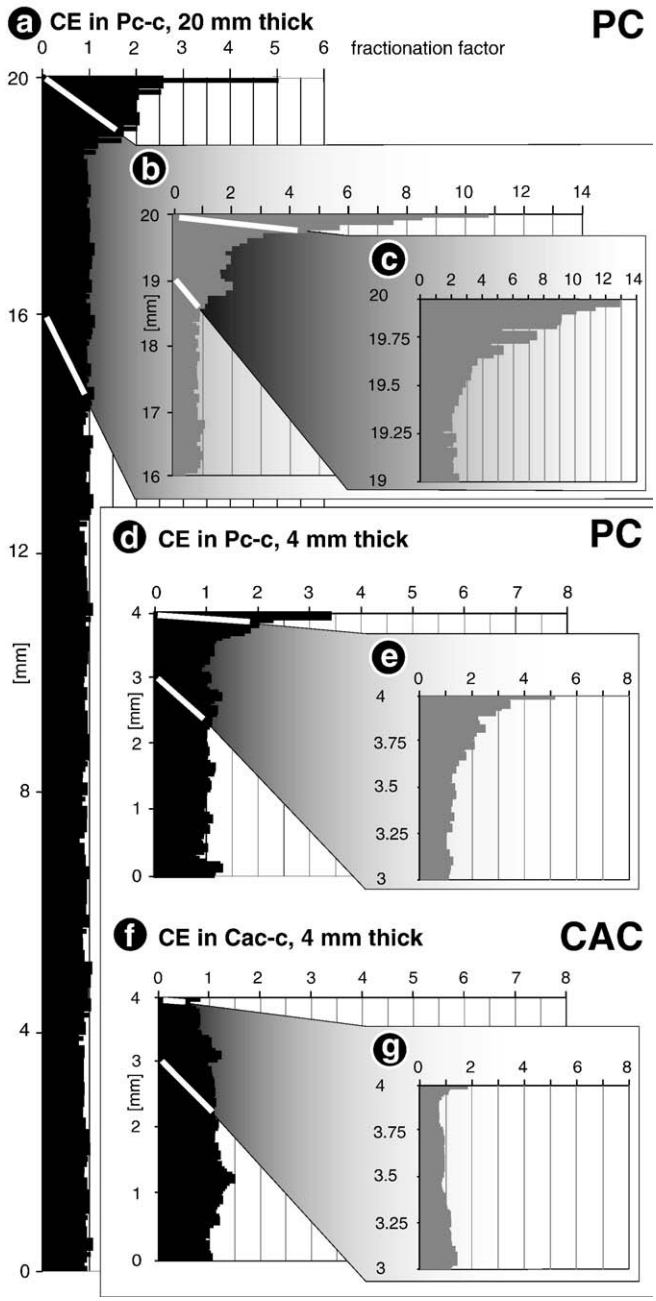

Fig. 6. Quantitative distribution diagrams of cellulose ether in ~20 mm thick PC dominated formulation (a–c), in 4 mm thick PC dominated (d, e) and in 4 mm CAC dominated (f, g) formulations. For further explanations see text.

is characterized by enrichment in PCE, CE, Cas and PVA. (iii) Below the ~1 mm thick upper part the distribution of organic additives is quite homogeneous.

A closer examination reveals additional differences in the distribution between the different additives. Latex (VC) shows no gradients throughout the mortar layer (Fig. 4a) except for an abrupt and strong increase up to a fractionation factor of 2.5 at the very mortar top (Fig. 4b). PCE reveals quite a homogeneous distribution with a minor skin enrichment (Fig. 5). CE distributions in the PC dominated thin and thick samples (Fig. 6a–e) show a homogeneous distribution in the lower part but an abrupt increase in the uppermost millimeter and the surface skin. In contrast, CE in the CAC dominated sample (Fig. 6f,g) is quite homogeneously distributed over the entire mortar layer. Only the blow up of the uppermost millimeter shows enrichment in the surface skin. The casein distributions in PC dominated thin and thick samples (Fig. 8a–e) show enrichments in the surface skin and distinct casein depletion in the underlying millimeter. In the CAC dominated formulation (Fig. 8f, g) the distribution is more even and the depletion below the surface does not exist. In the thin and thick PC dominated samples polyvinyl alcohol presents (Fig. 7a–e) a pronounced enrichment in the skin and the underlying millimeter, which continuously decreases towards the base of the mortar layer. The PVA distribution in the CAC dominated thin sample (Fig. 7f, g) shows a similar pattern but with an additional enrichment at 2 mm height and a distinct depletion at the base. Table 2 lists the fractionation factors of each of the additives in all three characteristic zones of the mortar layer.

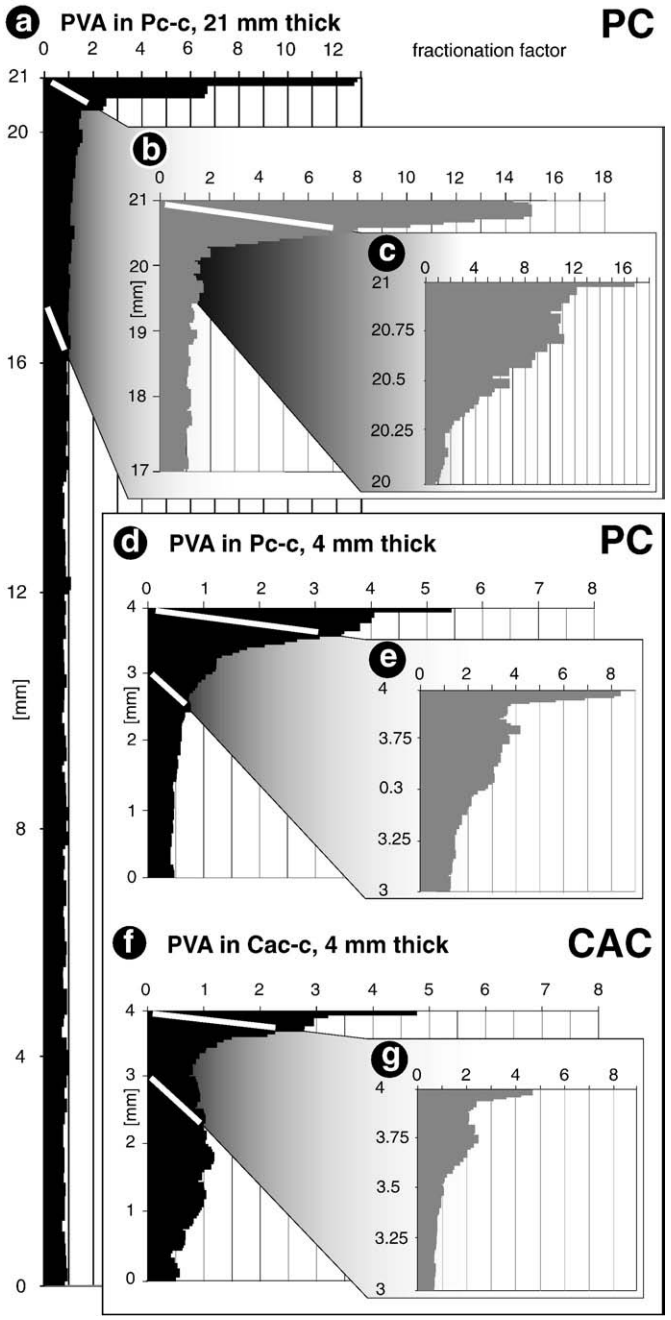

Fig. 7. Quantitative distribution diagrams of polyvinyl alcohol in ~20 mm thick PC dominated formulation (a–c), in 4 mm thick PC dominated (d, e) and in 4 mm CAC dominated (f, g) formulations. For further explanations see text.

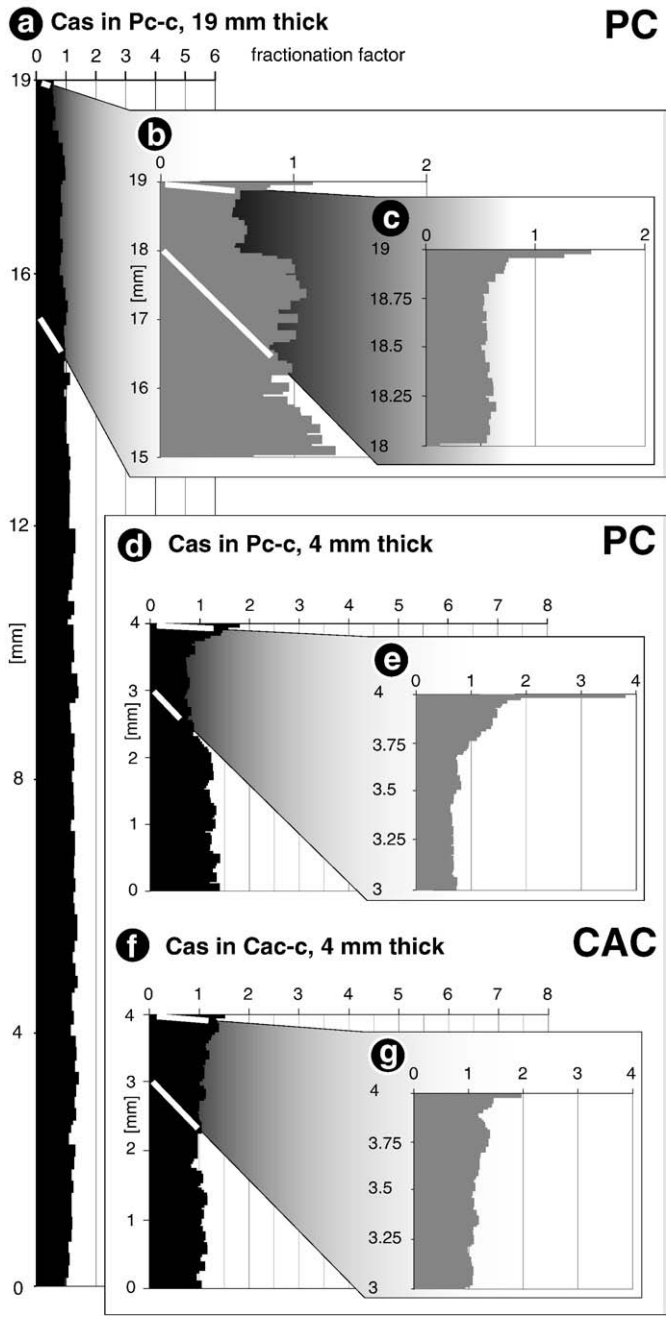

Fig. 8. Quantitative distribution diagrams of casein in ~20 mm thick PC dominated formulation (a–c), in 4 mm thick PC dominated (d, e) and in 4 mm CAC dominated (f, g) formulations. For further explanations see text.

4.4. Cellulose ether distribution in model mortar

Model mortars contain no cementitious phases (PC, CAC, Calcium sulfate). The goal of these experiments was to check, if the absence of cementitious phases has an effect on the distribution pattern of the organic additives i.e. on the related transport/enrichment processes.

The cellulose ether in the model mortar (Fig. 9a) shows a surface enrichment factor, which is higher than in all experiments containing cementitious phases. At the mortar/air interface a distinct skin developed. The blow up of the uppermost millimeter (Fig. 9b) reflects a considerable additive enrichment followed by an abrupt depletion towards the lower parts, which then show homogeneous CE distributions.

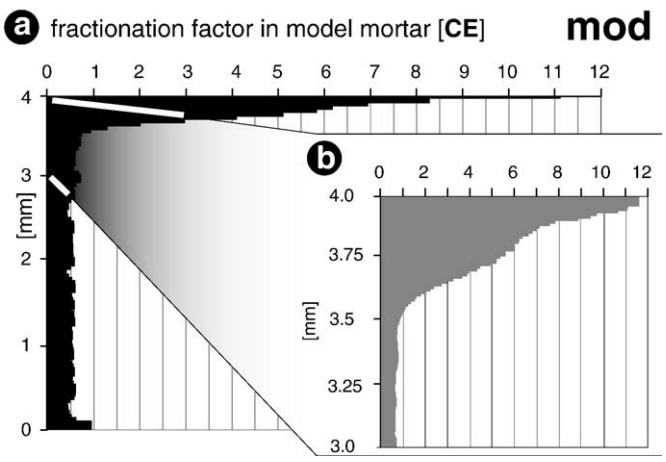

Fig. 9. Quantitative distribution diagrams of cellulose ether in a 4 mm thick model mortar layer.

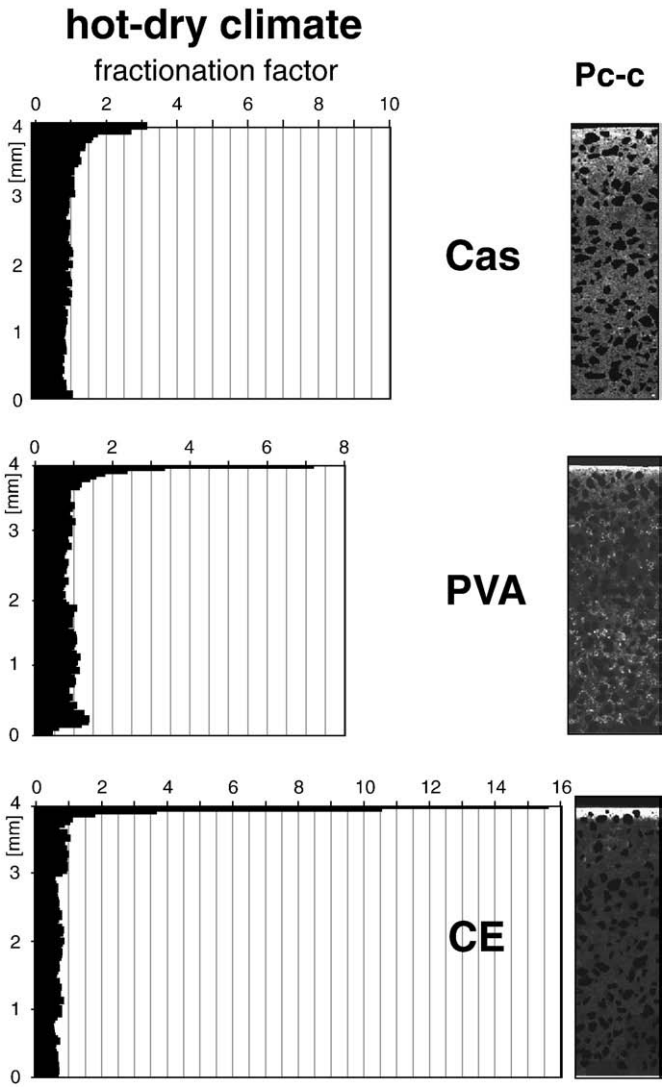

Fig. 10. The skin (i) of the samples cured under hot-dry climate conditions represent the zone with the most considerable additive enrichment. It seems that under these extreme climatic conditions Cas, PVA and especially CE are mobilized from zone (iii). Cas shows the lowest and CE the highest mobility due to strong evaporation.

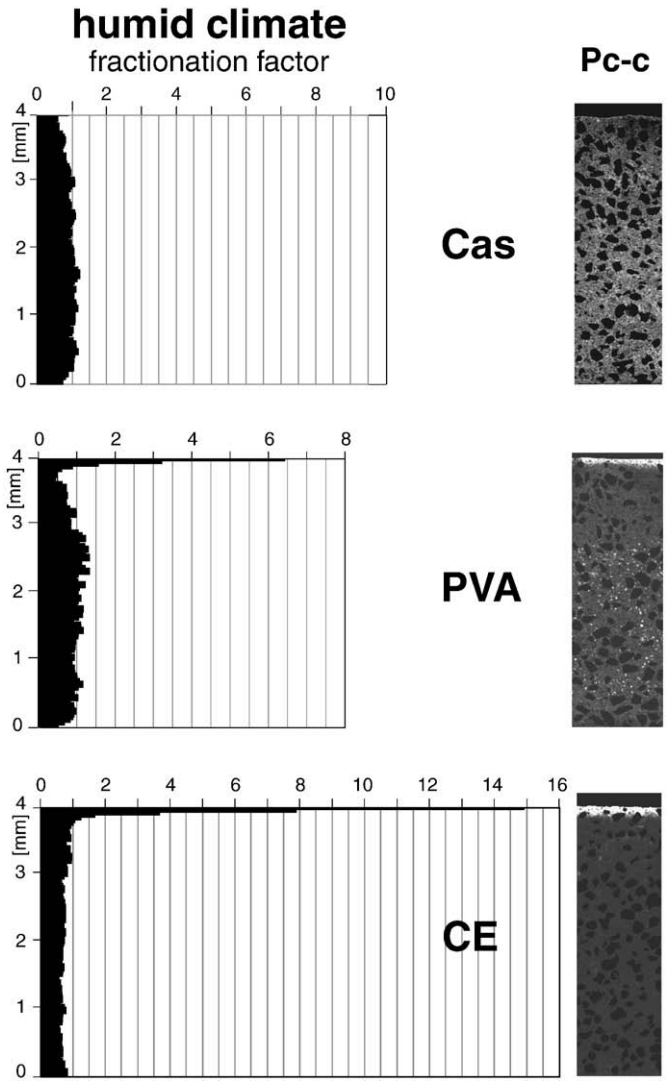

Fig. 11. Cas shows almost no fractionation in the mortar layer for humid curing conditions. PVA develops a strong skin (i) enrichment and a much lower and irregular distribution in zones (ii) and (iii). CE is characterized by a strong skin (i) enrichment and by low and homogeneous distributions in zones (ii) and (iii). Note that the samples were taken out of the climate box after 24 hours to let them dry under normal climate conditions.

4.5. Organic additive distribution as a function of the curing conditions

Evaporation plays an important role for the organic additive distribution in the mortar [1]. To improve the understanding of the influence of the evaporation rate onto the additive distribution, the mortar specimens were cured under 3 different climates: 23 °C/50% rel. humidity (referred to as normal climate (Figs. 4–9)), 50 °C/low humidity (referred to as hot-dry climate (Fig. 10)) and 23 °C/100% rel. humidity (referred to as humid climate (Fig. 11)). For the samples cured at humid climate (Fig. 11), it is important to mention that they were taken out of the climate box after 24 h to allow them to dry under normal climate conditions (see also Fig. 12).

According to the distribution profiles of cellulose ether, casein and polyvinyl alcohol three major zones can be distinguished: (i) the uppermost skin (0–10 μm) with highest additive concentration, (ii) a zone of about 1 mm in thickness, just below this skin with less pronounced enrichment (or even a depletion like in case of casein) and (iii) a zone, which begins at about 1 mm below the surface and reaches down to the base. The latter zone is slightly depleted in additive concentration.

The complete distribution profiles for the hot-dry climate are given in Fig. 10 and for the humid climate in Fig. 11. Table 2 displays the additive concentrations in terms of fractionation factors in the three major zones as a function of the normal, hot-dry and humid climates.

Table 2
Fractionation factors for CE, Cas, PVA, PCE and latex (VC) under the influence of different climatic curing conditions.

	CE			Cas			PVA			PVA	VC
	Normal	Hot-dry	Humid	Normal	Hot-dry	Humid	Normal	Hot-dry	Humid	Normal	Normal
0-0.1 mm	7.5	16	15	9	3	1	6.5	7	6.5	1.2	2.5
0.1 - 1 mm	2	1	1	0.6	1.3	0.9	1.5	1.1	0.7	1.0	2.0
1 - 4 mm	0.9	0.7	0.7	1.3	1	1.2	0.6	1	1.2	1.5	1.0

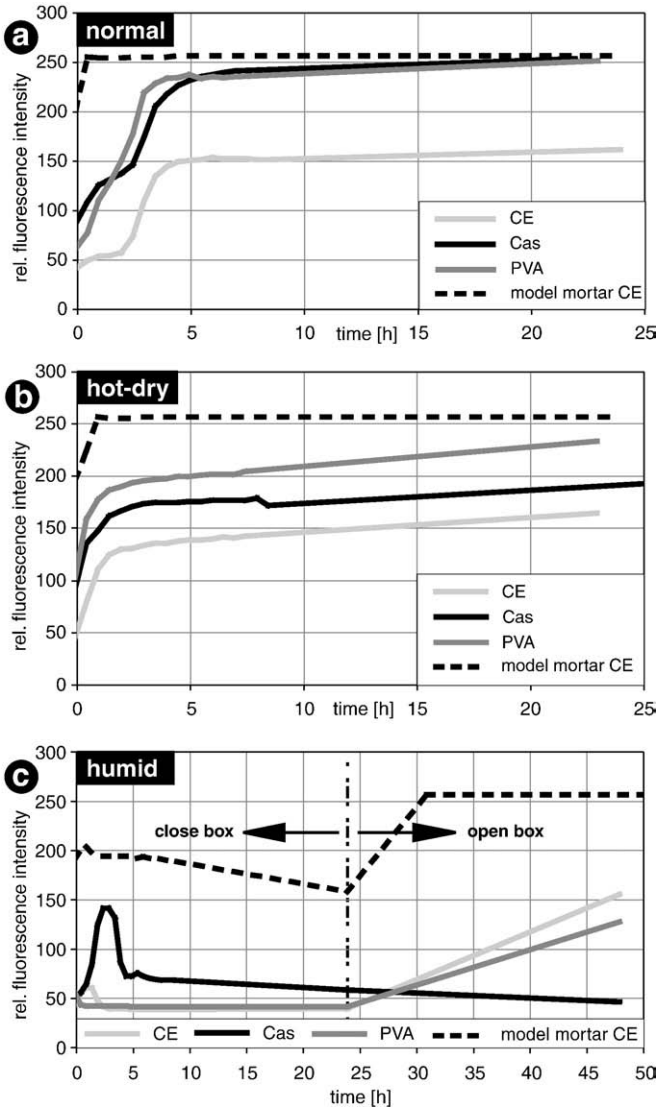

Fig. 12. The graphs show the development of the surface fluorescence intensity (FI) under normal (a), hot-dry (b) and humid (c) climatic conditions.

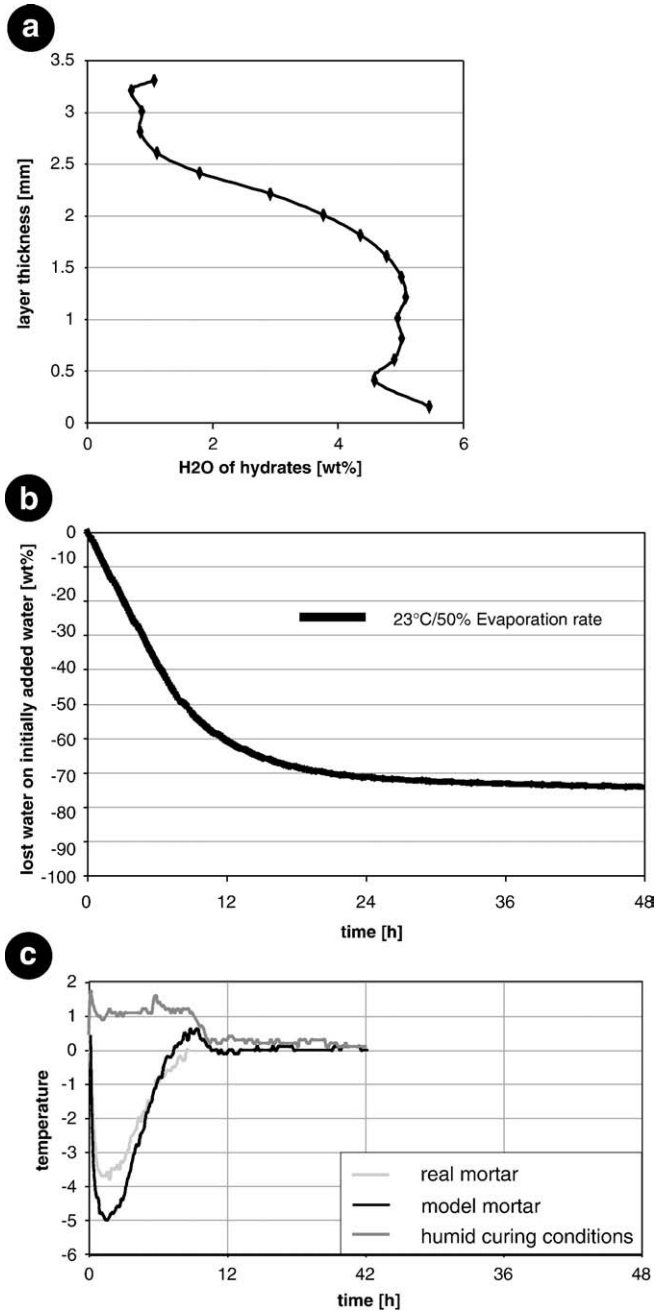

Fig. 13. Degree of hydration and changes in evaporation rate and temperature of a PC-dominated SLC. The ettringite distribution in (a) is measured with TGA along a vertical profile from top to base (method is described in the work of Jenni et al. [21]). The weight loss due to water evaporation is represented in (b). (c) shows the temperature development in the mortar for real and model mortars and for a mortar cured under humid conditions.

4.6. In-situ surface fluorescence intensity

For the mortar surface subjected to different curing conditions (normal, hot-dry, humid), Fig. 12 illustrates the development of the fluorescence intensity (FI) in time. It is important to keep in mind that by these experiments we only see the very surface, which corresponds in the cross-section (e.g. Figs. 4–11) to the topmost skin. Enrichments below the surface cannot be detected by in-situ surface observations. The FI development can be divided into three main phases: (i) the initial fluorescence, (ii) a fluorescence increase during the first 5–7 h and (iii) the long-term development up to one day.

4.6.1. Normal cured samples (Fig. 12a)

Stained CE in model mortar shows a high initial FI at the mortar surface that grows within 1 h to the maximum intensity, which is then constant during the next 24 h. In the real formulation, CE presents much lower FI values and the abrupt increase in FI is retarded by about 3 h. Casein reveals two stages of enhanced surface enrichment. One within the first hour while the second stage occurs simultaneous to CE enrichment. PVA enriches continuously during the first 3 h.

4.6.2. Hot-dry cured samples (Fig. 12b)

Under elevated rate of evaporation the enrichment of all additives at the surface is faster compared to the normal conditions, very similar for all additives and occurs relatively rapid within the first 2 h.

4.6.3. Humid cured samples (Fig. 12c)

During storage under humid conditions, all three additives show an initial enrichment subsequently followed by depletion. This phenomenon is most intense for Cas. However, the main enrichments of CE and PVA occur when evaporation is initiated by opening the box after 24 h of humid storage. Note that this enhanced evaporation does not affect Cas. These observations will have important implications for the interpretation of the final profiles of additive distribution within the SLCs cured under humid conditions (Fig. 11), as will be discussed below.

4.7. Ettringite evolution and distribution

Fig. 13a reveals TGA analyses of ettringite (method is described in [21]), which shows depleted and enriched zones, respectively, in the upper 1/3 and lower 2/3 of the PC-dominated SLC layer. The evaporation rate is nearly constant over the first 10 h and then levels out to result in a final value of 75% of the total amount of initially added water (Fig. 13b). Therefore only 25% of added water is chemically bound.

Due to the open system conditions, there is a distinct temperature evolution within the thin mortar bed (Fig. 13c). (i) During the first hour, the mortar temperatures of the real and model mortars decrease between 3 to 5 °C below room temperature. (ii) Then the mortar temperatures slowly rise to meet room temperature at about 7 h after application. Mortars cured under humid conditions (Fig. 13c), i.e. mortars with prevented evaporation, show a temperature increase of 1 °C during the first 10 h and afterwards a decrease to the room temperature.

5. Discussion

In the following discussion we will focus on the distribution of the organic additives (latex, PCE, CE, PVA, Cas) in the mortar layer as a function of different curing conditions, mortar thickness and the predominant cement type (PC vs. CAC). The additive distribution patterns are discussed in context of enrichment processes and hydration gradients (TGA data). All the results are schematically summarized in Fig. 14.

5.1. Influence of PC or CAC domination

Usually, the substrate is well primed before the SLC is applied. Therefore, water evaporation at the surface is the only mechanism, which can induce a significant water flow.

In the PC dominated formulations the enrichments of CE, Cas and PVA are twice as high as in the CAC dominated formulations. This could be explained by two factors: (a) different affinities of the organic additives to these cements and (b) different hydration rates.

(a) Plank and Winter [6] and Hirsch et al. [8] describe that the adsorption behavior of an additive is strongly selective with

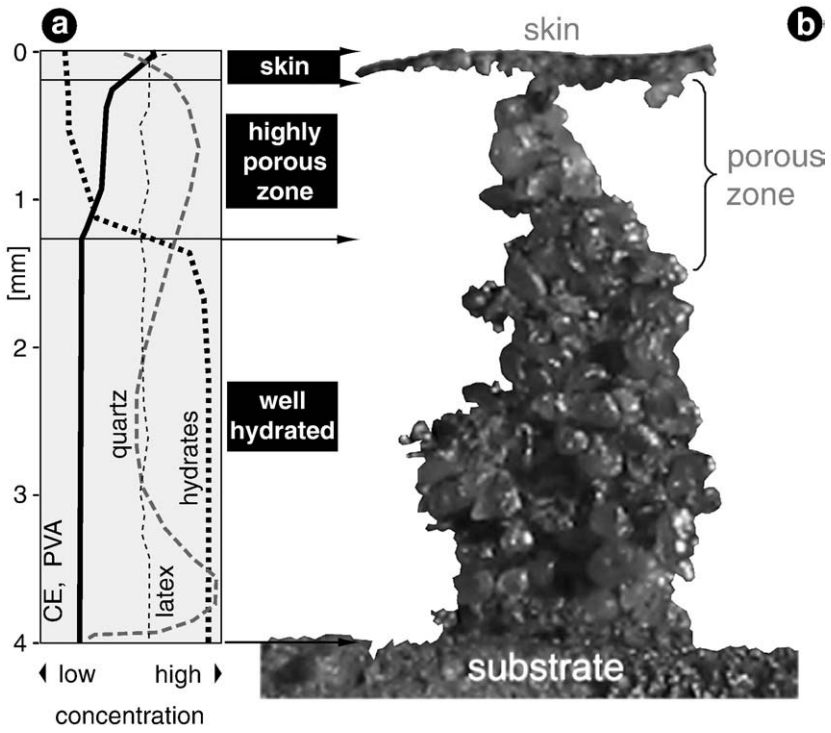

Fig. 14. Schematic summary of distribution patterns in the mortar layer. The left diagram (a) shows the final concentration profiles of CE, PVA, latex (VC), hydrates and quartz sand. Note that the mortar layer is subdivided into three distinct zones, (i) a skin (<100 μm), (ii) a partly hydrated zone with a high porosity (~100–1000 μm below surface), and (iii) a well hydrated basal zone. The image (b) represents these three zones in a mortar layer after hydrochloric acid treatment.

respect to different cement phases. Therefore, the predominance of PC or CAC would be expected to have an influence on the mobility of an additive. The fact that casein acts as a plasticizer implies a substantial adsorption on the mineral interfaces but apart from these general statements, specific adsorption data of the single additives on different clinker phases are lacking so far.

(b) PC dominated formulations hydrate slower and to a lesser extend. Therefore, they should have (i) bigger capillary pore sizes and the pore system would be expected to be connected over a longer time [25], (ii) a higher content of unbound free pore water and (iii) if the additives can be trapped by the growing ettringite [26], smaller amounts of ettringite in case of PC dominated formulations should result in higher concentrations of un-trapped free additive in the pore solutions. The explanation that the enrichment of water-soluble polymers is higher the lower the degree of hydration is confirmed by the distribution patterns of the sequence shown by Figs. 6g,e and 9b. Here a decreasing degree of hydration, which is even zero in the model mortar, results in maximum fractionation factors of 1.8, 5.1 and 11.5 at the mortar skin.

CAC is highly reactive and supports the growth of hydrates considerably. Ettringite growth, for example, consumes a substantial part of the mixing water and decreases the amount of free water already during an early stage of the fresh mortar. This reduces the water migration towards the surface. Due to the formation of ettringite the pore size is reduced and the total pore surface of the system is enlarged. In this way, the small-sized porosity acts like a filter and inhibits the movement of the large organic additives (e.g. Ø casein micelle ~100 nm). Note that due to ongoing hydration, the pores can be filled by hydrates, and that the consumption of pore water creates empty pores. Both processes interrupt the communication of the pore water system with the surface and therefore also the evaporation-induced migration of the pore water and therein dissolved ingredients. Additionally, chemical and physical drying go hand in hand with the start of the film formation of the organic additives [29,30], which induces larger particle sizes of the additives and an increase in viscosity of the remaining pore solution. This behavior additionally reduces the migration ability of the additives.

PCE (Fig. 5) and latex (Fig. 4) were only investigated in PC dominated systems. PCE shows strong adsorption behavior (Fig. 5; Table 2) to cementitious surfaces [31,6]. Once adsorbed it is extremely difficult to remove it from the mineral surfaces. This explains the very homogeneous distribution of PCE without a major concentration gradient. In contrast to solution polymers, redispersible powder is composed of micron-sized latex particles, which cannot pass the finest capillary pores. Therefore, their mobility is reduced and does not allow migration across the entire mortar layer. As a consequence, latex particles generally are homogeneously distributed throughout the matrix (Fig. 4; also compare [20]). However, note a distinct enrichment of latex in the skin (Fig. 4b), which is interpreted in relation to the formation of a water rich layer during the phase of defoaming. The drying of this water layer will then leave a skin rich in phases, which were previously dispersed and dissolve in it. For analytical reasons it was necessary to choose latex, which is not exactly designed for this application. This may explain the uneven chlorine distribution due to undispersed latex clusters (Fig. 4b).

5.2. Influence of cementitious phases

De Gasparo [1] demonstrated that the ionic strength of the pore water can partly suppress the fluorescence intensity. To avoid this artifact, reference measurements with a model mortar were carried out containing no cementitious ingredients. In fact, Fig. 12 shows that the initial fluorescence intensity (FI) of a model mortar is about twice as high than in case of real mortars. On the other hand, for the model mortar the additive enrichment occurs much earlier and faster, which can be attributed to the lack of hydration. As no hydrates are formed, only physical drying at the mortar/air interface causes the water loss in the system and the capillary pore size is not changed. The mobility

of the water-soluble additives is therefore increased (see discussion in previous section 5.1b). Slowing down in enrichment results by the steadily reduced amount of pore water. In this sense, the aforementioned plugging effect and enhanced viscosity induced by the additives may also contribute to the slow down in enrichment in case of real mortar systems.

5.3. Influence of mortar layer thickness (PC dominated)

The influence of mortar thickness (Figs. 6, 7 and 8a, b, c) on the distribution of CE, Cas and PVA was tested in Portland cement dominated formulations (Table 1). For the specific additives and mortar locations where the thin SLC layers show a zone of enrichment or depletion, there is also a corresponding zone of enrichment or depletion in case of the thick layers. Thus, the distribution patterns of the additives in thin and thick layers are generally quite similar. However, an important difference is that CE and PVA are significantly more fractionated if the layer is thicker, while in case of Cas the layer thickness does not affect the fractionation factors much. This indicates that CE and PVA are mobilized through the entire mortar layer. Hence, the thicker the layer, the bigger are the fractionation factors because larger amounts of additives can be mobilized. In case of Cas, the enrichment in the skin (<100 μm) seems only to create depletion in a 1 mm thick zone, which is right below the skin. This fractionation behavior seems not to be influenced by the layer thickness, indicating that Cas is quite immobile because it is generally adsorbed. However, some minor mobility seems to be given in the uppermost 1 mm, where the degree of hydration is low and, as a consequence, the porosity must be high and the amount of mineral interfaces small.

5.4. Surface fluorescence development under different curing conditions

In-situ FI observations of the surface generally confirm the final distribution patterns observed in cross-sections of hardened samples. However, some distinct differences in the results of these different experiments occur. The first 5 h of the normal and hot-dry cured samples confirm the hypothesis, that evaporation plays a key role for the enrichment process of water-soluble polymers (Fig. 12). Under normal conditions it takes about 4 h to reach the maximum fluorescence, whereas hot-dry conditions takes less than half of that time. In terms of the effect of the degree of hydration on the additive mobility, information can be directly obtained by comparing Fig. 12a with 12c, where the latter stage reflects a retarded onset of evaporation after 24 h of hydration. Fig. 12c indicates that after these 24 h of hydration, the mobility of CE is highest compared to PVA and Cas. However, closer examinations show that the rate of enrichment after these 24 h is four times slower compared to the rate of enrichment under normal and hot-dry climate conditions. As already mentioned above, this retardation can again be related to a denser mortar texture due to an increased degree of hydration and therefore a lower permeability.

5.5. Influence of normal, hot-dry and humid curing conditions

The climate experiments reveal the influence of different curing environments on the fractionation of the organic additive in 4 mm thick mortar layers (Figs. 6d, 7d, 8d, 10, 11). Except for Cas, hot-dry cured samples generally show higher skin enrichments compared to the normal cured samples. This can be explained with a higher evaporation rate. Macroscopic observations reveal that the mortar surface of hot-dry cured samples immediately develops a fine dry skin. It seems that in this skin, the concentrations of water-soluble polymers were enhanced while the water content decreased. It is known that under elevated temperature conditions [29] these polymers form films with inclusions of fine cementitious or carbonaceous crystals, which grew in-situ or were transported with the migrating pore water to the surface. These composite films at the mortar surface [21] are also found in case of SLCs, where they appear in the BE images as light grey structures [1,24].

The distribution pattern of humid cured 4 mm thin layers (Fig. 11) can be regarded as a measure how strongly the additives get immobilized during the first 24 h of humid curing conditions (closed climate box), when evaporation is not allowed. As final curing (after 24 h) took place under open climate box conditions, the usual migration processes related to drying became active. With this respect, we can conclude that CE and PVA did not loose their mobility and are still free to migrate in the mortar after 24 h. CE seems even to be better dissolved, as the mortar skin is more enriched in CE (Fig. 11c) than under normal curing conditions (Fig. 6d). This can be attributed to a complete hydrolysis of PVA under alkaline conditions of the mortar, which reduced its water solubility and therefore limits its resulting fractionation by the migrating pore water. Casein shows a very homogeneous distribution if cured the first 24 h under humid conditions (Fig. 11a). This indicates that casein must have lost its mobility during the first 24 h in the climate box due to adsorption and cement hydration (e.g. pore size reduction). Also the comparison between normal and hot-dry cured samples (Figs. 8d and 10a) shows a big sensitivity of casein distribution on the climate. Hot-dry curing conditions have accelerated the migration of casein from the lowermost area towards upper parts during a time where hydration was not very progressed. This results in a gradual enrichment from bottom to top. In contrast to this, under normal climate conditions a distinct zone (~1 mm thick) of depletion in casein is developed right underneath the casein-rich skin. The depletion in casein below the skin could be the result of varying hydration intensities in different mortar areas. Fig. 13a shows that the hydration is better developed in the lower half of the SLC layers. It is possible that the active hydration process in this area generates a downward flow of the free pore water, which contains the dissolved casein. In these deeper areas the continuous hydration generates new mineral surfaces, where casein gets immobilised by adsorption. However, the mortar surface is strongly enriched in casein due to evaporation driven water migration. In the case of hot-dry cured samples, evaporation is accelerated and dominates casein fractionation. The sample dries much earlier, before hydration-induced downward pore water flow would be able to transport non-adsorbed Cas towards deeper levels in the SLC.

6. Conclusions

The presented investigations allow the localization and quantification of quartz filler (Fig. 1), organic additives (Figs. 4–11) and ettringite (Fig. 13) in self-leveling compounds. Particularly the approach of selective additive staining in combination with in-situ observations of fluorescence development helps to gain new insights into the dynamics of a SLC during curing.

- The Quartz filler distribution can be rather complex and is based on combined effects of gravitational segregation and flow behavior during spreading.
- The water-soluble organic additives like cellulose ether, casein and polyvinyl alcohol are able to form films and are very sensitive to water migration processes, which influences their final distributions. Under normal curing conditions, all three additives finally are considerably enriched at the mortar surface (skin). Due to the size of latex particles (redispersible powder) and the high affinity of PCE to mineral surfaces, these two additives are more homogeneously distributed throughout the mortar layer. Hence, they were blocked in the matrix (latex) or adsorbed on cement surfaces already during an early stage of the evolving mortar and remained attached to these sites for the entire evolution, preventing a remobilization by the migrating water. However, the distinct enrichment of latex by a factor of 2 in the topmost skin might indicate an additional fractionation process

related to the formation of a water film at the surface during the phase of defoaming. Drying of this water film can macroscopically be observed and is generally referred as the end of gloss time. All ingredients dispersed and dissolved in the mortar water would then precipitate and form films creating a significant part of the skin.

- Rheology modifiers (all of the investigated additives are to adjust the rheological properties of the fresh mortar) become fractionated during hardening of the mortar layer and have a substantial influence on the final physical properties of the hardened mortar. Best example is casein, a classical plasticizer, which finally acts as a reinforcing additive increasing significantly surface hardness.
- The final distribution patterns strongly depend on the formulation, in particular on the type of the used mixed binder system (see Table 1). Portland cement dominated formulations react slower and less intensive. Therefore, the water consumption by the hydration reactions is weaker and the capillary pores are bigger. Both of these compositional and structural differences increase the mobility of water-soluble polymers. Thus, the surface enrichment of such polymers is much more pronounced in Portland cement dominated formulations compared to fast setting CAC dominated mixed binders.
- Curing under normal, hot-dry and humid conditions of samples (see Figs. 6–8, 10–12) with different layer thickness prove evaporation to be the key mechanism for the fractionation of water-soluble polymers. Samples cured under the influence of heat (enhanced rate of evaporation) show the strongest fractionations. This is confirmed by the observation that under humid conditions, where evaporation is stopped, fractionation is reduced (see Fig. 12c).
- Vertical fractionation of the water-soluble polymers and the degree of hydration reveal strong vertical gradients in compositions and microstructures. Thereby it was found that two major mechanisms are responsible for all these gradients, (i) evaporation and (ii) hydration.
  (i) Evaporation causes two important aspects, an upwards-directed flow of pore water and a downwards migrating drying front. Evaporation is, thus, the principle driving force for the generation of all gradients described above.
  (ii) Hydration consumes water and the hydrates grow in the capillaries reducing the amount and sizes of the latter. All together, hydration is the principle factor to reduce any of the gradients.

Conclusively, drying (mainly influenced by climatic conditions on the construction site) and hydration (mainly given by mortar formulation such as type of mixed binder and amount of polymer modifications) are counteracting processes, which will decide how self-leveling flooring compounds will finally perform. In light of a general comparison between PC and CAC dominated systems, the latter perform better. In detail, however, the performance of the SLCs strongly depends on the specific formulations, which can be designed for the purposes needed on the application site.

Acknowledgments

Our many thanks go to Verena Jakob, who overcame the demanding preparation of the numerous LSM samples. We would like to thank Thomas Aberle for the support of the organic additive staining. Financial support by the Swiss Commission for Technology and Innovation (6423.1 IWS-IW) and ELOTEX AG is gratefully acknowledged. We thank the Institute of Pharmacology in Berne for the uncomplicated use of their LSM facility.

References

[1] A. De Gasparo, Fractionation Behavior of Organic Additives and Resulting Microstructural Evolution of Mixed-Binder Based Self-Leveling Flooring Compounds, Thesis, Institute of Geological Science, Bern, Switzerland, 2006.
[2] L. Amathieu, A. Bier, K. Scrivener, Mechanisms of set acceleration of Portland cement through CAC addition, Int. Conf. on Calcium Aluminate Cement, Calcium Aluminates Cements, Edinburgh, 2001.
[3] Th.A. Bier, L. Amathieu, Calcium aluminate cement (CAC) in building chemistry formulations, CONCHEM congress, Ref. F 97, 1997.
[4] A. De Gasparo, J. Kighelman, R. Zurbriggen, K. Scrivener, M. Herwegh, Self-leveling flooring compounds: application, mechanisms and properties, China International Dry Mortar Production & Application Techniques Seminar, Beijing, 2006.
[5] R. Zurbriggen, E. Bühler, J. Lang, Mixed-binder based self-leveling flooring compounds: critical formulations — the reason for typical damages, ibausil, Weimar, 2006.
[6] J. Plank, C. Winter, Adsorption von Fliessmitteln an Zement in Gegenwart von Verzögerern, GDCh, vol. 27, 2005, p. 55.
[7] J. Plank, G. Bassioni, Z. Dai, H. Keller, B. Sachsenhauser, N. Zouaoui, Neues zur Wechselwirkung zwischen Zementen und Polycarboxylat-Fliessmitteln, ibausil, Weimar, vol. 1, 2006, pp. 579–598.
[8] C. Hirsch, D. Vlad, Y.J.-Y., P. Chatziagorastou, J. Plank, Adsorption von Fliessmitteln an Mineralphasen der frühen Zementhydratation, GDCh, vol. 27, 2003, p. 187.
[9] J.B. Kazirukanyo, N. Tenoutasse, Investigation of the interactions between superplasticizers and C3A, C4AF and calcium sulfoaluminates through the adsorption mechanism, 14. ibausil Conference, Weimar, vol. 1, 2000, p. 357.
[10] A. Brandl, D. Vlad, Kompetitive Adsorption von anionischen Zusatzmitteln am Beispiel Fliessmittel - Verzögerer - Wasserretentionsmittel, GDCh Bauchemie-Tagung, Erlangen, 2004.
[11] P. Wang, G. Zhang, Study on physical properties of some dry mortars, 15. Internationale Baustofftagung, Weimar, vol. 2, 2003, pp. 0323–0330.
[12] C.-J. Häcker, M. Arnold, Einfluss von Celluloseethern auf die Zementhydratation, ibausil, Weimar, vol. 1, 2006, pp. 607–614.
[13] A. Dimmig, Einflüsse von Polymeren auf die Mikrostruktur und die Dauerhaftigkeit kunststoffmodifizierter Mörtel (PCC), Bauhaus-Universität Weimar, Weimar, 2002.
[14] M.U.K. Afridi, Z.U. Chaudhary, Y. Ohama, K. Demura, M.Z. Iqbal, Effects of polymer modification on the formation of high sulphoaluminate or ettringite-type (AFt) crystals in polymer-modified mortars, Cement and Concrete Research 24 (8) (1994) 1492–1494.
[15] M.U.K. Afridi, Y. Ohama, K. Demura, Morphology of $Ca(OH)_2$ in polymer-modified mortars and effect of freezing and thawing action on its stability, Cement and Concrete Composites 12 (3) (1990) 163–173.
[16] O. Rozenbaum, R.J.-M. Pellenq, H. Van Damme, An experimental and mesoscopic lattice simulation study of styrene-butadiene latex–cement composites properties, Concrete Science and Engineering 37 (2004).
[17] J. Kighelman, K. Scrivener, R. Zurbriggen, Effect of the mix binder system on the hydration of self-leveling compounds, ibausil, Weimar, 2006.
[18] H.J. Weyer, I. Müller, B. Schmitt, D. Bosbach, A. Putnis, Time-resolved monitoring of cement hydration: influence of cellulose ethers on hydration kinetics, Nuclear Instruments and Methods in Physics Research B 238 (2005) 102–106.
[19] L. Amathieu, B. Valdelièvre, Calcium aluminate cement: a versatile binder for various applications in the dry mortar industry, 2004 China International Dry Mortar Production & Application Techniques Seminar, China, 2004.
[20] A. Jenni, M. Herwegh, R. Zurbriggen, T. Aberle, L. Holzer, Quantitative microstructure analysis of polymer-modified mortars, Journal of Microscopy 212 (2003) 186–196.
[21] A. Jenni, L. Holzer, R. Zurbriggen, M. Herwegh, Influence of polymers on microstructure and adhesive strength of cementitious tile adhesive mortars, Cement and Concrete Research 35 (2005) 35–50.
[22] A. Jenni, M. Herwegh, R. Zurbriggen, L. Holzer, Sample preparation of polymer-modified high-porous mortars for quantitative microfabric analysis, in: B. Georgali (Ed.), Proceeding of the 8th Euroseminar on Microscopy Applied to Buildings Materials, 2001, pp. 571–578.
[23] F.W.D. Rost, Quantitative Fluorescence Microscopy, Cambridge University Press, Cambridge, 1991.
[24] A. De Gasparo, H. Herwegh, R. Zurbriggen, Methods to unravel the distribution of polymers during the evolution of self-leveling flooring compounds (SLC), 10th Euroseminar on Microscopy Applied to Building Materials, 2005, Paisley.
[25] J. Kighelman, Hydration and Structure Development of Ternary Binder System as Used in Self-Levelling Compounds, École Polytechnique Fédérale de Lausanne, EPFL, Switzerland, Lausanne, 2007.
[26] J. Pourchez, Aspect physico-chimique de l'interaction des éthers de cellulose avec la matrice cimentaire, Ecole Nationale Supérieure des Mines de Saint-Etienne, Saint-Etienne, 2006.
[27] B. Möser, Nano-Charaktrisierung von Hydratphasen mittels Rasterelektronenmikroskopie, 15. Internationale Baustofftagung, Weimar, vol. 1, 2003, pp. 0589–0607.
[28] M. Langenfeld, J. Stark, Frühe Hydratation von Portlandzement unter Zusatzmitteleinfluss - dargestellt im ESEM-FEG, EDO-Tagung, F.A.F.I. Bauhaus-Universität, Saarbrüücken, 1998.
[29] T. Jahr, Untersuchung der Filmbildung aus Polymerdispersionen mit Hilfe der forcierten Rayleighstreuung, Johannes Gutenberg-Universität, Mainz, 2002.
[30] S. Cramer, Filmbildung industrieller Latices: Anwendung von ESR-Spin-Sonden-Methoden, Universität Mainz, Mainz, 2001.
[31] J. Plank, C. Hirsch, C. Winter, P. Chatziagorastou, Neues zur Wirkungsweise von Polycarboxylat-basierten Fliessmitteln, ibausil, Weimar, vol. 1, 2003, pp. 1393–1408.